Organic & Biomolecular Chemistry

ROYAL SOCIETY OF CHEMISTRY

PAPER

View Article Online
View Journal | View Issue

Cite this: *Org. Biomol. Chem.*, 2023, **21**, 5117

Seven-membered ring nucleobases as inhibitors of human cytidine deaminase and APOBEC3A†

Harikrishnan M. Kurup, [a,b] Maksim V. Kvach, [a] Stefan Harjes, [a] Geoffrey B. Jameson, [a,b] Elena Harjes *[a,b] and Vyacheslav V. Filichev *[a,b]

The APOBEC3 (APOBEC3A-H) enzyme family as a part of the human innate immune system deaminates cytosine to uracil in single-stranded DNA (ssDNA) and thereby prevents the spread of pathogenic genetic information. However, APOBEC3-induced mutagenesis promotes viral and cancer evolution, thus enabling the progression of diseases and development of drug resistance. Therefore, APOBEC3 inhibition offers a possibility to complement existing antiviral and anticancer therapies and prevent the emergence of drug resistance, thus making such therapies effective for longer periods of time. Here, we synthesised nucleosides containing seven-membered nucleobases based on azepinone and compared their inhibitory potential against human cytidine deaminase (hCDA) and APOBEC3A with previously described 2′-deoxyzebularine (dZ) and 5-fluoro-2′-deoxyzebularine (FdZ). The nanomolar inhibitor of wild-type APOBEC3A was obtained by the incorporation of 1,3,4,7-tetrahydro-2*H*-1,3-diazepin-2-one in the TTC loop of a DNA hairpin instead of the target 2′-deoxycytidine providing a K_i of 290 ± 40 nM, which is only slightly weaker than the K_i of the FdZ-containing inhibitor (117 ± 15 nM). A less potent but notably different inhibition of human cytidine deaminase (CDA) and engineered C-terminal domain of APOBEC3B was observed for 2′-deoxyribosides of the *S* and *R* isomers of hexahydro-5-hydroxy-azepin-2-one: the *S*-isomer was more active than the *R*-isomer. The *S*-isomer shows resemblance in the position of the OH-group observed recently for the hydrated dZ and FdZ in the crystal structures with APOBEC3G and APOBEC3A, respectively. This shows that 7-membered ring analogues of pyrimidine nucleosides can serve as a platform for further development of modified ssDNAs as powerful A3 inhibitors.

Received 12th March 2023,
Accepted 22nd May 2023

DOI: 10.1039/d3ob00392b

rsc.li/obc

1. Introduction

The enzymes of the polynucleotide cytidine deaminase family of APOBEC3 (A3A-H except E) form an important part of the immune system. By hypermutating cytosine to uracil in single-stranded (ss)DNA and RNA (Fig. 1A), A3 enzymes target viruses[1] and retrotransposons.[2] However, several enzymes, particularly A3A, A3B, A3H and A3G, can deaminate cytosine in human nuclear and mitochondrial genomes.[3] Viruses and cancer cells use this mutational activity of A3 proteins to escape adaptive immune responses, and become drug resistant[4–8] leading to poor clinical outcomes. Of the seven A3 enzymes, three (A3A, A3B and A3H) are localised in the cell nucleus and are genotoxic in unfavourable situations. Overexpression of A3A and A3B leads to tumourigenesis in transgenic mouse models.[9,10] Initially, A3B was identified as the primary source of DNA mutations in breast and other cancers,[6,7,11] but more recent research also points to a prominent role of A3A in cancers.[12–14] Since A3A and A3B are not essential to primary human metabolism and A3B deletion is prevalent in some populations,[15] their inhibition offers a useful strategy to suppress cancer evolution and thereby make the existing anti-cancer therapies more efficient.[7,16] As A3 enzymes deaminate predominantly ssDNA, we have been exploring the possibilities of ssDNA-based inhibitors that can be used as conjuvants to existing cancer therapies.[17–19]

Despite low sequence identity, cytidine deaminase (CDA) and A3 share a similar overall structural topology and close structural homology for the Zn^{2+}-containing active site. Consequently, these enzymes are believed to have a similar mechanism of cytosine deamination. The major difference

[a]*School of Natural Sciences, Massey University, Private Bag 11 222, Palmerston North 4442, New Zealand. E-mail: e.harjes@massey.ac.nz, v.filichev@massey.ac.nz*
[b]*Maurice Wilkins Centre for Molecular Biodiscovery, Auckland 1142, New Zealand*

†Electronic supplementary information (ESI) available: Experimental details of the synthesis of nucleosides and modified oligodeoxynucleotides and enzymatic assays; and the sequence alignment of proteins used in this study, ^{1}H, ^{13}C, ^{31}P NMR, IR and HRMS (ESI) spectra of new compounds synthesised, RP-HPLC profiles and HRMS (ESI) spectra of oligodeoxynucleotides. CCDC 2207173 and 2207174. For ESI and crystallographic data in CIF or other electronic format see DOI: https://doi.org/10.1039/d3ob00392b

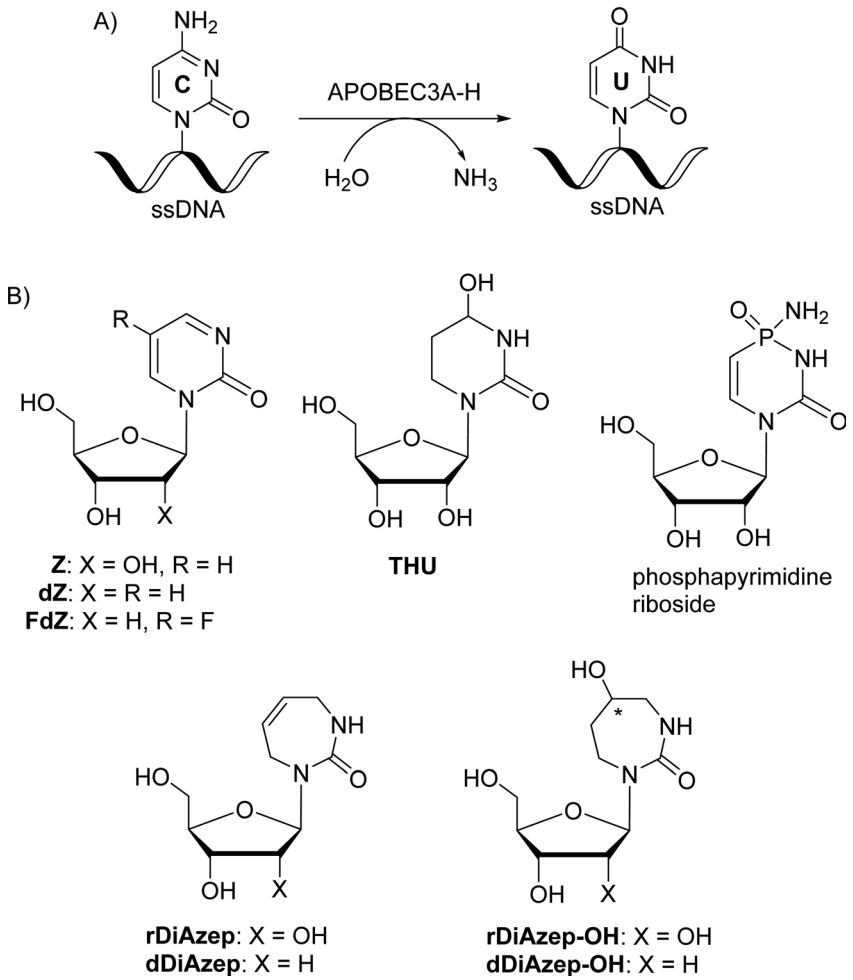

Fig. 1 (A) Deamination of dC in ssDNA by A3 enzymes. (B) Previously described powerful CDA inhibitors.

between them is that CDA accepts only individual nucleosides as substrates, whereas A3s act mainly on ssDNA having at least four nucleotides, one of which is 2'-deoxycytidine.[20]

CDA is a key enzyme of primary metabolism that catalyses the deamination of cytidine or 2′-deoxycytidine to uridine or 2′-deoxyuridine, respectively.[21,22] The spontaneous deamination of cytidine is a very slow process; the accelerated rate of deamination by the enzyme is through the formation of a hydrated intermediate species.[23] CDA forms a part of the pyrimidine salvage pathway and full inhibition of CDA leads to accumulation of toxic pyrimidine catabolism intermediates.[24,25] However, several cytosine-based chemotherapeutics such as cytarabine,[26] gemcitabine[27] and decitabine[28] have been shown to be deaminated by CDA in the liver and spleen, which reduces their potency. Local and temporary inhibition of CDA in these organs is therefore a useful strategy that can mitigate detrimental degradation of chemotherapeutics. In July 2020, a combination of the known CDA inhibitor cedazuridine, (4*R*)-2′-deoxy-2′,2′-difluoro-3,4,5,6-tetrahydrouridine,[29] and decitabine as an oral pill (C-DEC or ASTX727) developed by Astex Pharmaceuticals was approved by the US Food and Drug Administration (FDA) for the treatment of patients with intermediate/high-risk myelodysplastic syndromes (MDS) and chronic myelomonocytic leukemia (CMML).[30]

The most powerful inhibitors of CDA based on nucleosides described so far are 1,3-diazepin-2-one riboside (**rDiAzep**, Fig. 1B),[31–36] phosphapyrimidine riboside (unstable in water),[37] tetrahydrouridine (THU)[38] and zebularine (Z).[39,40] We demonstrated that the use of 2′-deoxy analogues of zebularine (dZ) and 5-fluorozebularine (FdZ) instead of dC in the preferred ssDNA substrate motif resulted in competitive inhibitors of A3.[17–19] Recently, we have shown that cross-linking of two distant nucleotides at +1 and −2 positions resulted in a more powerful dZ-containing A3A inhibitor than the linear ssDNA.[41] DNA hairpins with short loops have also been shown to provide selective inhibitors of A3A when the target dC in the loop was changed to dZ-derivatives.[42–44] We also demonstrated that dZ and THU as free nucleosides did not inhibit A3 enzymes, which indicates that ssDNA delivers dZ into the active site of A3.[17]

In the past, the diazepinone riboside was described as a more powerful inhibitor of CDA than dZ (K_i = 25 nM for 1,3-diazepin-2-one[31–35] and 2.9 μM for dZ).[45] Hence, we decided to expand a series of 2′-deoxy nucleoside analogues of CDA

inhibitors[31,34,46] used in ssDNA for A3 inhibition and investigate 1,3-diazepin-2-one riboside (**dDiAzep**) and its hydrated derivatives (**dDiAzep-OH**)[31–35] in this context.

2. Results and discussion

2.1. Structural considerations for the use of 1,3-diazepin-2-one nucleoside as an A3 inhibitor

The difference in the inhibitory potential of dZ and FdZ against $A3B_{CTD}$ and A3A[19] prompted us to investigate the possibility of the synthesis and incorporation of more powerful CDA inhibitors for the creation of more powerful A3 inhibitors.

Out of all the reported potent CDA inhibitors, 1,3-diazepin-2-one riboside[31–35] is notably different structurally as it has no functionality at C5 to coordinate with Zn^{2+} or to undergo hydration in the active site of CDA. In the crystal structure of 1,3-diazepin-2-one riboside with human CDA (hCDA, PDB ID: 1MQ0),[35] the protein self-associates to form a dimer of dimers (tetramer) (Fig. S2 in the ESI†) which is known to be active.[19] Each subunit is bound to one molecule of diazepinone riboside but each active site is made up of three of the four hCDA monomers and all of them contribute to the recognition of the inhibitor. It is interesting that diazepinone is not coordinated to Zn^{2+}. Instead, a water molecule is bound to Zn^{2+}. The nucleobase N3–H is engaged in interactions with Glu67 of hCDA and the oxygen of the carbonyl C2=O is hydrogen bonded to the main chain NH of Ala66 of the first subunit. The seven-membered nucleobase is puckered and the C5–C6 double bond of the molecule is involved in a canonical π–π interaction with Phe137 residue of the *third* subunit of hCDA. Reduction of the double bond to the corresponding saturated nucleoside led to significant loss in binding affinity to CDA which highlights the importance of the double bond for the inhibition of hCDA.[31] Interestingly, aromatic amino acids Tyr130 and Tyr313 are present at the same position in the active site of monomeric A3A and $A3B_{CTD}$, respectively, instead of Phe137 in hCDA (Fig. 2). We hypothesised that a π–π interaction between the double bonds of diazepinone and Tyr130 (A3A)/Tyr313(A3Bctd) will be preserved for A3A and A3B and potentially result in potent inhibition of these enzymes by diazepinone. These observations make this compound interesting to be synthesised as a 2′-deoxy analogue (**dDiAzep**, Fig. 1B) for testing as an A3 inhibitor when incorporated into ssDNA.

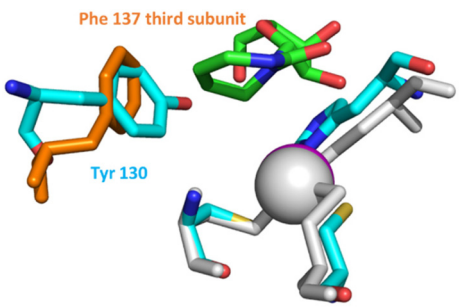

Fig. 2 Active site residues (grey) and diazepinone riboside (green) of hCDA (1MQ0) overlaid with the active site of A3A (5KEG) (cyan). Tyr 130 (cyan) of A3A is on the same place as Phe 137 (orange) of hCDA interacting with diazepinone; $zinc^{2+}$ atoms are shown as spheres. Structures were overlaid in pymol. The CDA tetramer is shown in ESI Fig. S2.†

To mimic the respective tetrahedral substrate intermediate in the context of 7-membered ring nucleobase, diazepinone derivatives carrying an OH-group on carbon C5 have been prepared as *R* and *S* isomers in the past (**rDiAzep-OH**, Fig. 1B).[31] One of the isomers was identified as a slow-binding inhibitor of CDA, as potent as THU. Unfortunately, the authors were unable to determine which isomer was more potent. The lack of proper stereochemical information prompted us to attempt the synthesis, isolation, and characterisation of the stereochemistry of both **dDiAzep-OH** isomers before their incorporation into ssDNA as A3 inhibitors.

2.2. Synthesis of modified 2′-deoxynucleosides, their DMT-protected phosphoramidites and derived oligodeoxynucleotides

2.2.1. Synthesis of dDiAzep phosphoramidite. The synthesis of a 2′-deoxy analogue of diazepinone riboside (**dDiAzep**) was based on a previously reported linear strategy of creating a nucleobase, 1,3-diazepin-2-one, on the sugar by using ring-closing metathesis (RCM) reaction on bis-allyl urea.[34,47,48] The synthesis started with the formation of bis-allyl urea **2** by the condensation of allylamine **1** in the presence of *N*,*N*-disuccinimidyl carbonate in THF (Scheme 1). Coupling of urea **2** with Hoffer's chlorosugar was performed by the previously described silyl modification of the Hilbert–Johnson reaction[49] using $SnCl_4$ as a Lewis acid in dichloroethane at −35 °C to result in the linear nucleoside **3** with moderate yield (47%) and a β : α ratio of 9 : 1. The β isomer as the major product was confirmed by a NOESY NMR experiment. The spectrum shows cross-peaks of the 1′ and 4′-protons of the major isomer of compound **3** through space, confirming it as a β-nucleoside, whereas the minor α-anomer had a cross-peak between the 1′ and 3′-protons (see Fig. S3 in the ESI†).

As reported in the literature, acylation of the amide **3** was required to lock the allyl groups in a *cis* orientation for the successful RCM.[47] The amide **3** was protected with benzoyl chloride to provide compound **4**. The subsequent RCM with the GreenCat™ catalyst provided the required seven-membered ring **5** in 41% isolated yield. Resuspending and washing the precipitate **5** in methanol gave a >99% pure β anomer. The toluoyl groups on compound **5** were selectively deprotected with a solution of aqueous ammonia in methanol followed by selective protection of the 5′-hydroxyl group using standard DMT protection conditions to provide compound **6** in 82% yield. Phosphoramidite **7** was prepared using standard phosphitylation conditions with an isolated yield of 82%.

The fully deprotected nucleoside, dDiAzep (**8**), was obtained by the deprotection of compound **5** in concentrated aqueous ammonia and isolated by preparative thin-layer chromatography (TLC) in 58% yield.

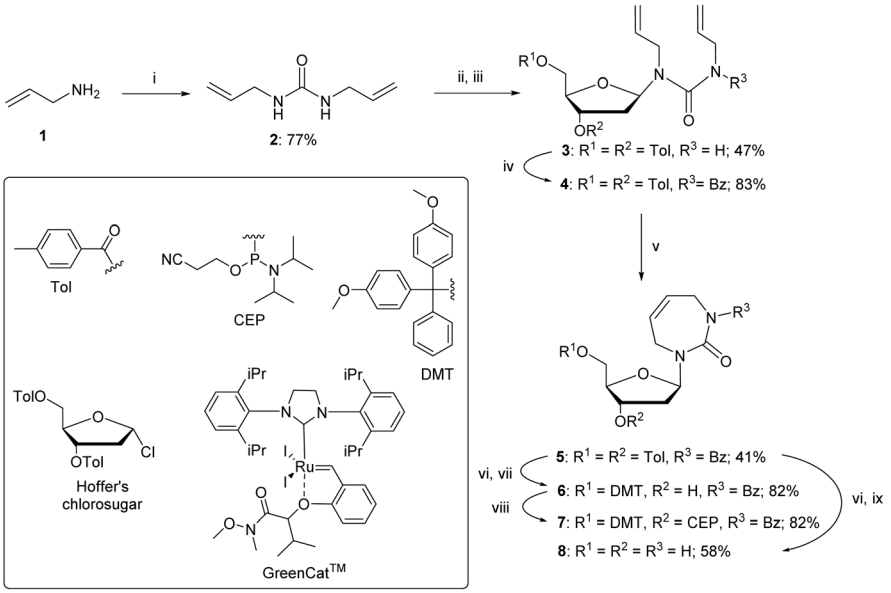

Scheme 1 Synthesis of 2′-deoxy diazepine phosphoramidite. Reagents and conditions: (i) *N*,*N*′-disuccinimidyl carbonate, THF, r.t., 2 h; (ii) TMS chloride, Et_3N, benzene, r.t., overnight; (iii) Hoffer's chlorosugar, $SnCl_4$, 1,2-dichloroethane, −35 °C, 1 h; (iv) benzoyl chloride, pyridine, 0 °C → r.t., overnight; (v) GreenCat™, dry DCM, reflux, 2 h; (vi) 30% aq. NH_3, MeOH (1 : 10, v/v), r.t., 3 days; (vii) 4,4′-dimethoxytrityl chloride (DMTCl), pyridine, 0 °C → r.t., overnight; (viii) *N*,*N*-diisopropylamino-2-cyanoethoxychlorophosphine (CEP-Cl), Et_3N, dry DCM, 0 °C, 20 min; and (ix) 30% aq. NH_3, r.t., 15 min.

2.2.2. Design and synthesis of modified *R*- and *S*-dAzep phosphoramidites. After the successful synthesis of compound **5** we planned to synthesise the 2′-deoxy form of the reported nucleoside **9** as a mixture of *R* and *S* isomers (Scheme 2). We investigated the possibility of a one-pot hydroboration/oxidation of the double bond as reported previously on 1,3-diazepin-2-one[32] followed by the removal of all the protecting groups. Unfortunately, the standard hydroboration/oxidation with BH_3·THF followed by H_2O_2/NaOH did not yield the required product **9** (Scheme 2); instead, two compounds were isolated. NMR analysis revealed that the double bond in the 7-membered ring was intact but one of the carbonyls was reduced to CH_2 and the sugar ring was present in an open chain form. The analysis of mass-spectroscopy data was not conclusive. We were unable to crystallise these compounds and determine their structure.

The above failed reaction on substrate **5** prompted us to investigate the possibility of hydroboration/oxidation on a protected nucleobase **12**. We started the synthesis with the previously obtained bis-allyl urea **2**. Benzoyl protection of the compound **2** followed by *tert*-butyloxy carbonyl (boc) protection allowed the facile RCM of compound **11** producing the protected nucleobase **12** in 50% overall yield over three steps. The attempted hydroboration/oxidation protocol resulted only in benzoyl deprotection. Next, we tried the same hydroboration/oxidation protocol on a free nucleobase **14** which was reported previously for the synthesis of compound **15**.[32] Unfortunately, the reported procedure did not work in our study and the starting material was isolated (Scheme 2). In the past this protocol was not chosen for the synthesis of the target **rDiAzep-OH**. Instead, the formation of a diastereomeric mixture of ribosides of *R*- and *S*-5-hydroxy-diazepin-2-ones (Fig. 3A) relied on the use of toxic mercury salts ($HgO/HgBr_2$) and perhydro-1,3-diazepine-2,5-dione that has to be synthesised.[31]

We envisioned that a potent CDA and A3 inhibitor can be based on the nucleoside carrying 1,3-diazepine-2-one in which the N3 atom is replaced with CH_2. One should note that the IUPAC nomenclature assignment of *R* and *S* isomers is opposite for 1,3-diazepin-2-one and azepin-2-one (Fig. 3).

The synthesis started from commercially available 1,4-cyclohexanedione cyclic ethylene monoketal (**16**) that was converted to oxime and then, using a Beckmann rearrangement, provided the required protected nucleobase as a 7-membered cyclic amide (**17**).[50] This compound was coupled with Hoffer's chlorosugar[51] in the presence of K-^{t}BuO in 1,4-dioxane at room temperature to provide the required nucleoside **18** with a β : α ratio of 99 : 1 as determined by NOESY NMR. However, deprotection of the ketal in compound **18** under various acidic conditions failed. The difficulties of deprotecting the cyclic ketal in 7-membered ring compounds have been reported in the past.[32] To circumvent these difficulties, we decided to change the synthetic route (Scheme 3) and rely on the benzyl-protecting group on the alcohol at C5 of the hexahydro azepin-2-one (**21**).

A pathway reported in the current paper includes the synthesis of the protected azepan nucleobase **21** from the cyclic ketal **16** using the Beckmann rearrangement on oxime **20** (Scheme 3).[50] The cyclic amide **21** and Hoffer's chlorosugar were coupled in the presence of K-^{t}BuO in 1,4-dioxane at room temperature to provide a pair of diastereomers **22*R*** and **22*S*** in moderate yields (47 and 24%, respectively) and a β : α ratio of

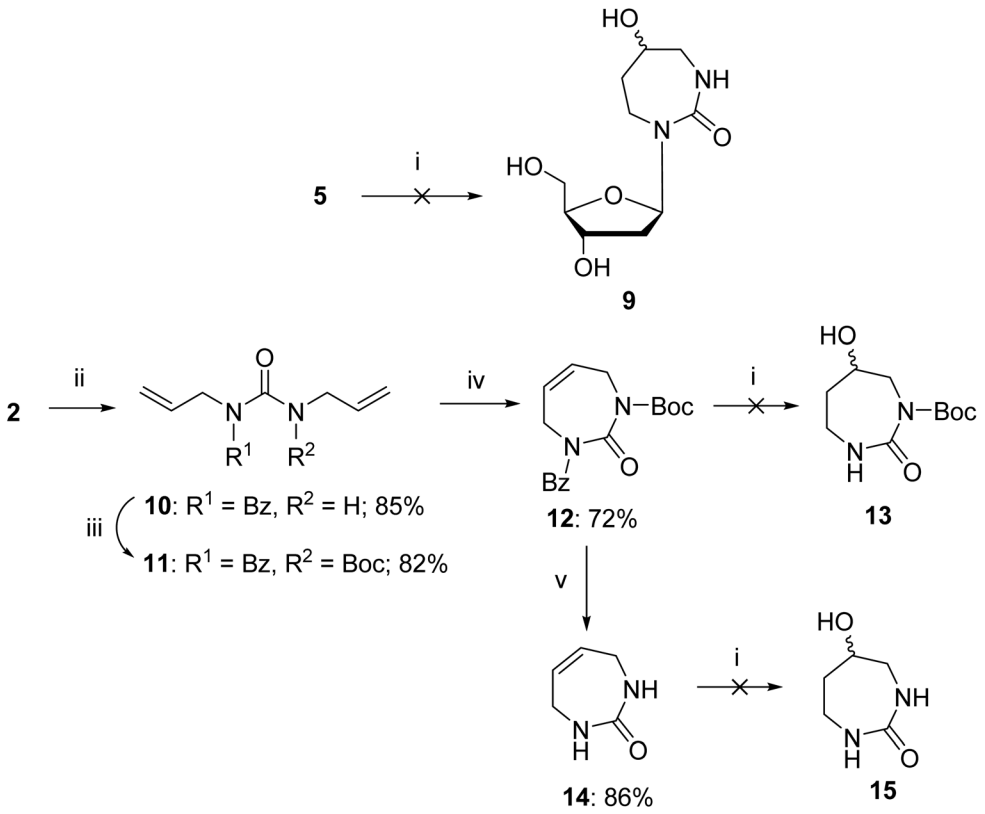

Scheme 2 Attempted hydroboration/oxidation of 1,3-diazepin-2-one nucleoside and nucleobase. Reagents and conditions: (i) 1 M BH_3·THF, 0 °C → r.t., 2.5 h, H_2O, 1 N NaOH, 30% H_2O_2, r.t., 1 h; (ii) benzoyl chloride, pyridine, 0 °C → r.t., overnight; (iii) Boc-anhydride, DMAP, Et_3N, THF, reflux, overnight; (iv) GreenCat™, dry DCM, reflux, 2 h; (v) 30% aq. ammonia in MeOH (1 : 10, v/v), 15 min then TFA, DCM, 15 min.

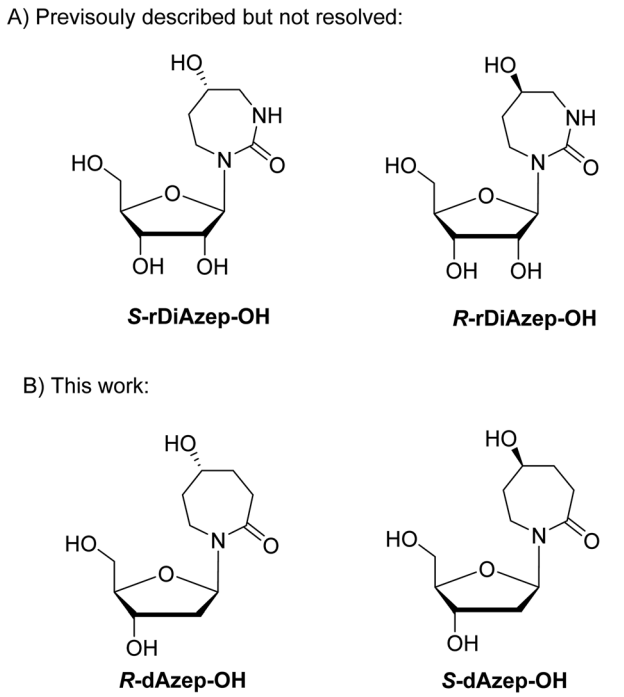

Fig. 3 (A) Previously described ribosides of *R*- and *S*-5-hydroxy-1,3-diazepin-2-ones. (B) Proposed structure of 2′-deoxyribosides of 5-hydroxy-azepin-2-ones.

99 : 1. These diastereomers were purified using silica gel column chromatography and crystallised. The stereochemistry of each compound was assigned based on X-ray crystal data (Fig. 4). Here onwards, these diastereomers were subjected to the same sequence of reactions separately. Benzyl deprotection of **22** was performed by catalytic hydrogenation using 10% Pd/C at room temperature to give **23*R*** and **23*S*** with 93 and 88%, respectively. One part of the benzyl-deprotected compounds was treated with 30% aq. NH_3 in MeOH at r.t. for 3 days to provide free nucleosides **24*R*** and **24*S*** with 72% and 79% yield, respectively, for evaluation as inhibitors of hCDA. The rest of each compound was protected with *tert*-butyl diphenylsilyl (TBDPS). After the removal of toluoyl groups, 5′-*O*-DMT-protected 3′-*O*-phosphoramidites **28*R*** and **28*S*** were prepared employing standard protocols.

We incorporated the modified nucleosides at the location of dC in the preferred A3 substrate motifs. Detailed procedures for oligodeoxynucleotide synthesis are provided in the ESI.† All oligodeoxynucleotides were purified by reverse-phase HPLC with detection at 260 nm. ESI-MS (Table 1) confirmed their compositions.

2.3. Evaluation of modified diazepinone derivatives as inhibitors of human CDA, engineered APOBEC3B and wild-type APOBEC3A

2.3.1. Evaluation of hCDA inhibition. Modified nucleosides **24*R*** and **24*S*** synthesised in current work were evaluated

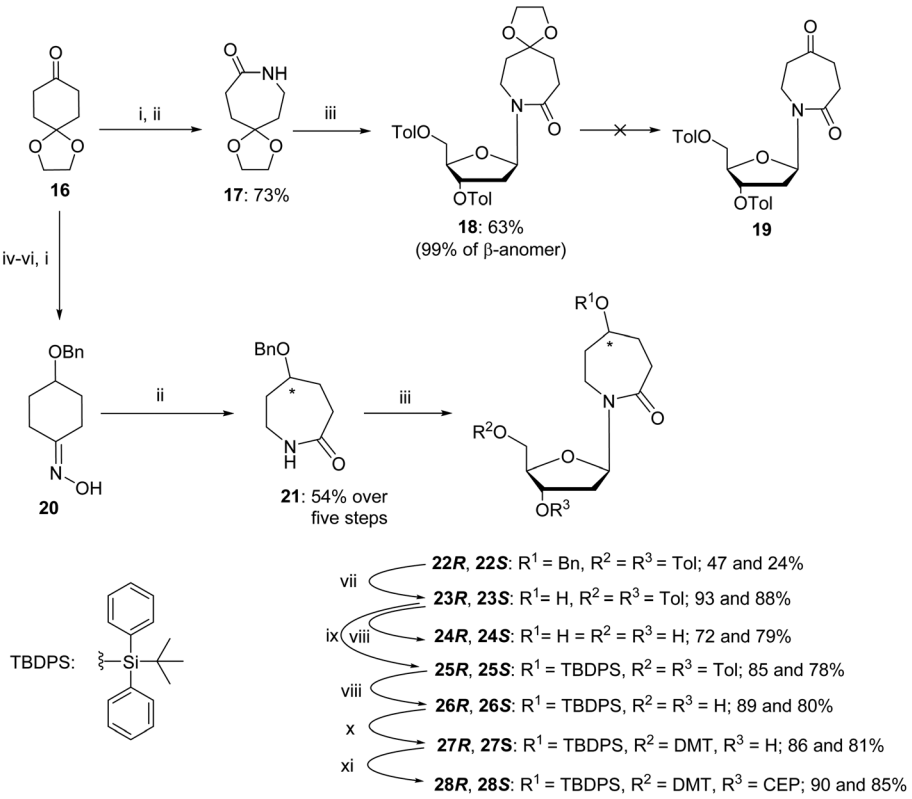

Scheme 3 Synthesis of ***R***-and ***S*-dAzep** nucleosides. Reagents and conditions: (i) $NH_2OH{\cdot}HCl$, NaOH, H_2O, MeOH, r.t., 10 min; (ii) tosyl chloride, 4N NaOH, acetone/H_2O r.t., 2 h then 4 N HCl, r.t., overnight; (iii) Hoffer's chlorosugar, K-^{t}BuO, 1,4-dioxane, r.t., 2 h; (iv) $NaBH_4$, MeOH, 0 °C → r.t., overnight; (v) benzyl chloride, Et_3N, DMF, 0 °C → r.t., overnight; (vi) 1 N HCl, THF, r.t., overnight; (vii) 10% Pd/C, H_2, EtOH, r.t., 6 h; (viii) 30% aq. NH_3, MeOH, r.t., 3 days; (ix) TBDPS chloride, imidazole, DCM, 0 °C → r.t., overnight; (x) 4,4′-dimethoxytrityl chloride (DMTCl), pyridine, 0 °C → r.t., overnight; and (xi) *N*,*N*-diisopropylamino-2-cyanoethoxychlorophosphine, Et_3N, DCM, r.t., 20 min.

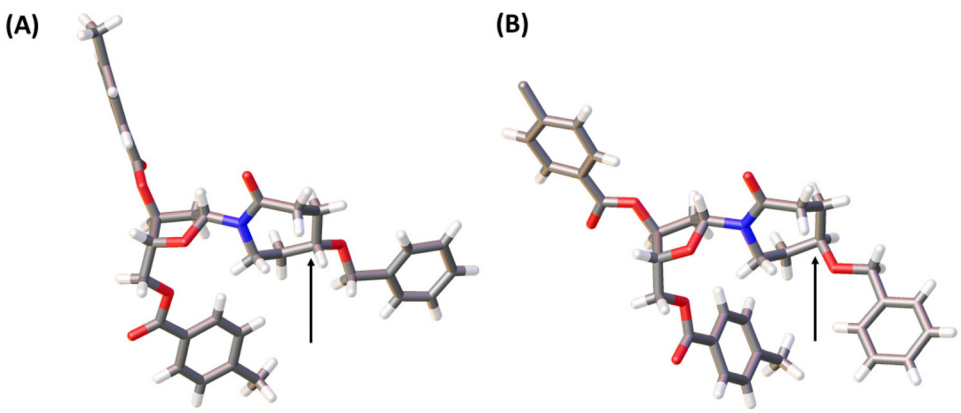

Fig. 4 X-ray structures of **22*S*** (A) and **22*R*** (B). Arrows indicate the stereocenters of these compounds where they differ. The structures have been deposited with the CCDC with deposition numbers 2207174 (**22*S***) and 2207173 (**22*R***).†

for their inhibition potential against hCDA by a UV-Vis based deamination assay described previously.[36] The deamination of dC leads to a decrease in absorption at 286 nm over time at pH 6.0 and 25 °C. **dZ** nucleoside was used as a positive control. As the original ***R***- and ***S*-rDiAzep-OH** nucleosides were reported as slow-binding inhibitors, our corresponding 2'-deoxy derivatives were also preincubated with hCDA for 5 minutes and then 100 μM substrate (dC) was added to start the measurements (Fig. 5).

By analysing the initial rate of deamination, we observed that the *S*-isomer of **24** was more potent than the *R*-isomer at all inhibitor concentrations with and without preincubation

Table 1 List of oligodeoxynucleotides synthesised as inhibitors of A3 enzymes

Name	DNA sequence, 5′ → 3′	Retention time[a] (min)	ESI-MS [Da], found/calculated
7-mer dZ-linear	TTTT **dZ** AT	14.2	2045.37/2045.37
9-mer dDiAzep	ATTT **dDiAzep** ATTT	15.9	2679.48/2678.50
7-mer *R*-dAzep-OH	TTTT ***R*-dAzep-OH** AT	14.9	2078.39/2078.41
7-mer *S*-dAzep-OH	TTTT ***S*-dAzep-OH** AT	14.8	2078.38/2078.41
FdZ-hairpin	$(GC)_2$TT **FdZ** $(GC)_2$	14.3	3311.50/3310.60
dDiAzep-hairpin	T$(GC)_2$TT **dDiAzep** $(GC)_2$T	14.3	3916.65/3916.69
S-dAzep-OH-hairpin	T$(GC)_2$TT ***S*-dAzep-OH** $(GC)_2$T	14.0	3934.65/3933.71

[a] Reverse-phase HPLC on a 250/4.6 mm, 5 μm, 300 Å C18 column (Thermo Fisher Scientific) using a gradient of CH_3CN (0 → 20% for 20 min, 1.3 mL min^{-1}) in 0.1 M TEAA buffer (pH 7.0) with detection at 260 nm.

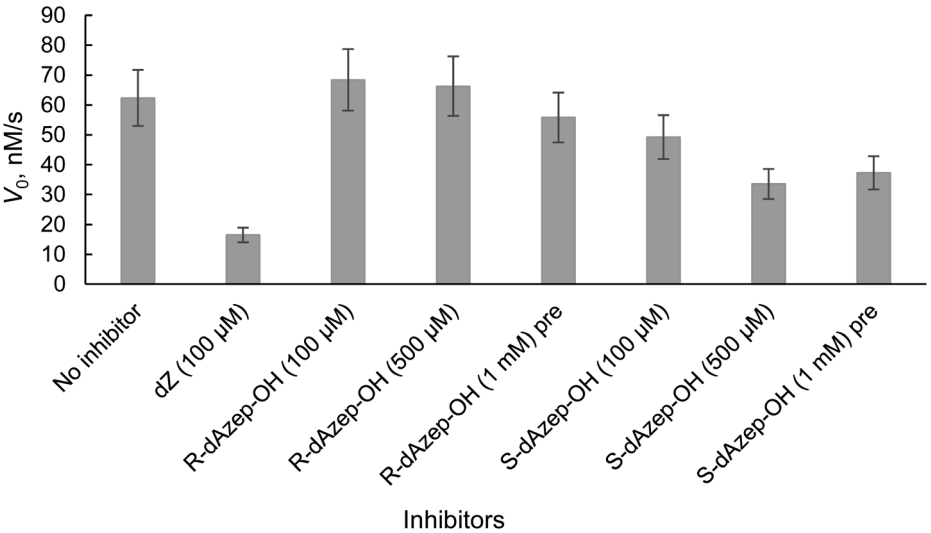

Fig. 5 Initial rate of hCDA-catalysed deamination of dC with and without inhibitors. Conditions: 100 μM dC as a substrate at specified concentrations of inhibitors, 27 nM hCDA, pH 6.0 at 25 °C. Measurements were taken at 286 nm. The suffix "pre" means that these samples were preincubated with hCDA for 5 min.

with hCDA. However, both analogues were not as powerful hCDA inhibitors as the previously described **dZ**. Therefore, no detailed analysis was performed. Instead, we focused our attention on the 1,3-diazepin-2-one 2′-deoxyriboside **8**.

The 1,3-diazepin-2-one riboside was previously reported as a powerful inhibitor of CDA. In order to accurately compare the 2′-deoxy form of 1,3-diazepin-2-one riboside and **dZ** we monitored the deamination of dC at 286 nm and analysed the kinetic profiles at various inhibitor concentrations using a global regression analysis of the kinetic data using Lambert's W function.[52] This method provides better estimates for K_m and V_{max} than non-linear regression analysis of the initial rate or any of the known linearised transformations of the Michaelis–Menten equation, such as Lineweaver–Burk, Hanes–Woolf and Eadie–Hofstee transformations.[52] Then the Michaelis–Menten constant (K_M) for the substrate and the inhibition constant (K_i) for each inhibitor were calculated (Table 2) assuming a competitive nature of inhibitors.

Indeed, **dDiAzep** nucleoside is an at least 20 times more powerful inhibitor of hCDA than **dZ** if K_m/K_i values are compared. This warrants evaluation of **dDiAzep** incorporated in ssDNA as an inhibitor of A3 enzymes.

Table 2 K_m of the substrate dC and K_i of dZ and **dDiAzep** against hCDA

Inhibitor	K_m of dC[a] (μM)	K_i (μM)	K_m/K_i
dZ	260 ± 40	10.7 ± 0.5	24
dDiAzep, **8**	220 ± 80	0.43 ± 0.08	512

[a] K_M was fitted in each experiment independently (see the ESI†).

2.3.2. Evaluation of diazepinone derivatives as inhibitors of engineered A3B$_{CTD}$ by ^{1}H-NMR assay. We used the ^{1}H NMR assay to test our short oligodeoxynucleotides containing 7-membered ring inhibitors of CDA as inhibitors of A3. This real-time NMR assay is a direct assay; it uses only A3 enzymes and oligodeoxynucleotides in a suitable buffer system, unlike many fluorescence-based assays where a secondary enzyme and a fluorescently modified oligodeoxynucleotide are used.[53] The NMR-based assay yields the initial velocity of deamination of various ssDNA substrates, including the modified ones,[18] in

the presence of A3 enzymes. Consequently, the Michaelis–Menten kinetic model is used to characterise substrates and inhibitors of A3. The modified nucleotides were incorporated instead of the target dC in the preferred DNA motif (TCA) of A3A and A3B on linear DNA. A previously described A3 inhibitor 5′-T_4**dZ**AT (7-mer-dZ) was used as a control.[17–19] The engineered A3 enzyme used in our initial experiments is the well-characterised and active derivative of the C-terminal domain of A3B ($A3B_{CTD}$), called $A3B_{CTD}$-QM-ΔL3-AL1swap,[17] where loop 3 is deleted and loop 1 is replaced with the corresponding loop 1 from A3A (the full protein sequence is provided in Fig. S1 in the ESI†). The residual activity of $A3B_{CTD}$-QM-ΔL3-AL1swap on the unmodified oligodeoxynucleotide (5′-T_4CAT) as a substrate in the presence of a known concentration of inhibitors was measured using the NMR assay (Fig. 6).

The results revealed that to achieve a similar level of inhibition induced by 7-mer-dZ we had to increase the concentration of oligodeoxynucleotides containing azepinone nucleotides from 8 to 36 μM. Despite the fact that **dDiAzep** was a more powerful inhibitor of hCDA in comparison with **dZ**, it did not exhibit a similar effect on engineered $A3B_{CTD}$. Interestingly, the inhibition by ***R*-dAzep-OH** and ***S*-dAzep-OH** containing oligodeoxynucleotides was poor compared to the standard inhibitor (7-mer-dZ), but the difference in the inhibitory potential observed between ***R*** and ***S*** isomers was similar to that seen for hCDA (Fig. 5). This suggests the orientation of –OH on the nucleobase which mimics the intermediate formed after the attack of H_2O at C4 of cytosine by $A3B_{CTD}$-QM-ΔL3-AL1swap.

2.3.3. Evaluation of DNA-hairpins containing diazepinone derivatives as inhibitors of wild-type A3A. Recently, it was reported that A3A binds to DNA hairpins[54,55] and prefers deaminating cytosines present in the short loops of DNA hairpins rather than linear DNA at pH 7.[56] To evaluate diazepinone derivatives as A3A inhibitors, we introduced **dDiAzep** and ***S*-dAzep-OH** instead of the target dC in a DNA hairpin with a TTC loop. All inhibitors were tested in the ^{1}H NMR assay monitoring A3A-catalysed deamination of dC-hairpin ($T(GC)_2TTC(GC)_2T$, where bold C is deaminated) at 150 mM salt concentration and pH 7.4. For comparison, we used the best linear oligodeoxynucleotide described so far against $A3B_{CTD}$-QM-ΔL3-AL1swap, FdZ-linear (AT_3**FdZ**AT_3)[19] and a DNA-hairpin containing **FdZ**, $(GC)_2TT$**FdZ**$(GC)_2$.[43] Deamination data were analysed using Lambert's W function as described in the ESI.† The calculated inhibition constants are provided in Table 3.

The K_i values show that **FdZ** and **dDiAzep**-containing hairpins are superior inhibitors of the wild-type A3A in comparison with the best linear oligodeoxynucleotide (FdZ-linear). It is also evident from these data that **FdZ** and **dDiAzep** are more potent inhibitors of A3 when used instead of dC in the structure of the hairpin than in the linear 9-mer sequence (Fig. 6

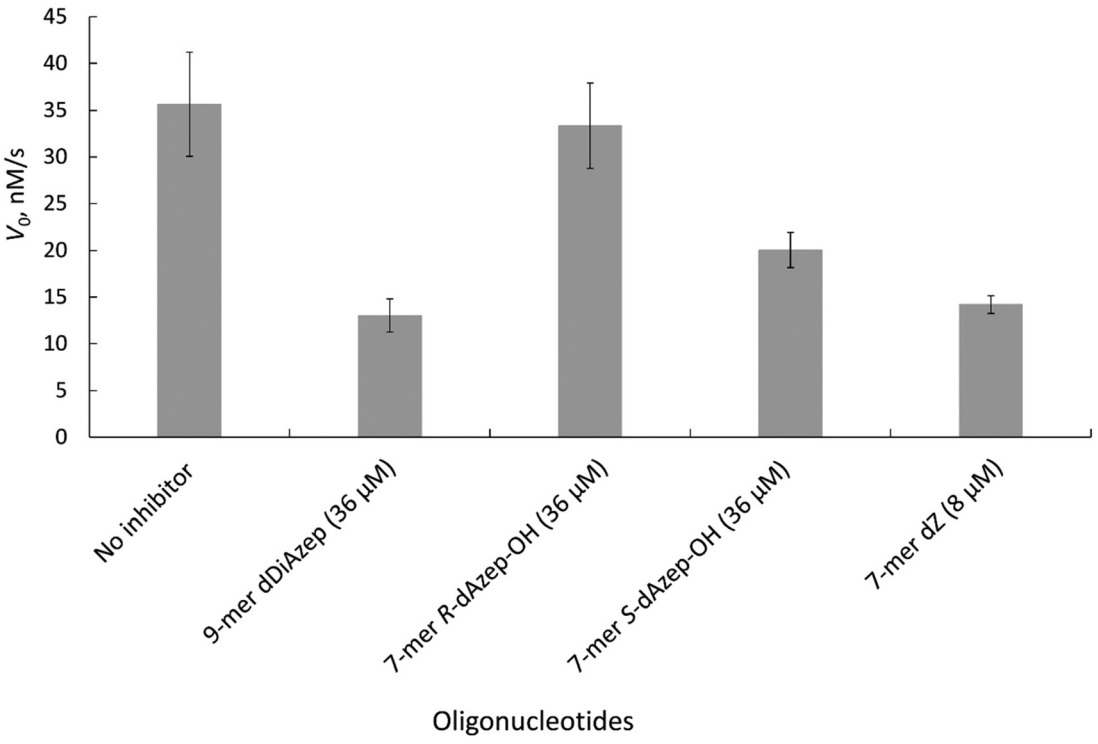

Fig. 6 Initial rate of $A3B_{CTD}$-QM-ΔL3-AL1swap-catalysed deamination of 5′-T_4CAT in the absence (no inhibitor) and presence of inhibitors at the concentrations indicated. Conditions: 400 μM 5′-T_4CAT, 36 μM seven-membered ring containing oligodeoxynucleotides and 8 μM **dZ**-containing oligodeoxynucleotide, 300 nM $A3B_{CTD}$-QM-ΔL3-AL1swap in a 50 mM sodium phosphate buffer (pH 6.0) containing 100 mM NaCl, 2.5 mM β-mercaptoethanol, 50 μM 3-(trimethylsilyl)-2,2,3,3-tetradeuteropropionic acid (TSP) and 20% D_2O at 25 °C. Error bars are estimated standard deviations from triplicate measurements.

Table 3 K_i values of inhibitors of wild-type A3A

Inhibitor	K_i (nM)
FdZ-linear	2400 ± 940
FdZ-hairpin[43]	117 ± 15
dDiAzep-hairpin	290 ± 40
***S*-dAzep-OH**-hairpin	6000 ± 1000

Conditions: 50 mM Na^+/K^+ phosphate buffer, pH 7.4 supplemented with 100 mM NaCl, 1 mM TCEP, 100 μM DSS and 10% D_2O at 20 °C; enzyme concentration: 140 nM; substrate concentration (dC-hairpin): 500 μM. K_m for the dC-hairpin against A3A is 21 ± 10 μM (ref. 43) (33 ± 7 μM in experiments with the ***S*-dazep-OH**-hairpin). Full structural characterisation of the FdZ-hairpin in the complex with A3A and the activity of the FdZ-hairpin in cells will be published elsewhere.[43]

and Table 3). A hairpin carrying ***S*-dAzep-OH** instead of dC has a K_i of 6 μM which is worse than the K_i for FdZ-linear. These data support our assertion that nucleoside-like inhibitors of CDA can be converted into inhibitors of A3 when used instead of dC in a DNA hairpin.

3. Discussion

A3 enzymes catalyse the deamination of cytosine to uracil in ssDNA substrates, thus playing a key role in innate antiviral immunity. However, the A3 family has also been linked to many mutational signatures in cancers, which sparked our interest in developing inhibitors of A3's catalytic activity as potential therapeutics and tools to study the biochemistry, structure and cellular function of these enzymes.

Recently, we have shown that the incorporation of cytosine-like 2′-deoxyzebularine[45,57] and 5-fluoro-2′-deoxyzebularine (**dZ** and **FdZ** on Fig. 1B) into short, linear ssDNA led to the first selective A3 inhibitors[17–19] with low micromolar inhibition constants (K_i). We have proposed that the inhibitory potential of ssDNAs can be further improved through the incorporation of more potent inhibitors of CDA into ssDNA.[19] Here we have considered several diazepin derivatives known to inhibit CDA and incorporated them into ssDNA as possible inhibitors of A3 enzymes. It was pleasing to note that the RCM methodology allowed us to obtain and evaluate diazepinone 2′-deoxyriboside (**dDiAzep**, Fig. 1B) as an inhibitor of hCDA, engineered $A3B_{CTD}$ and A3A. In comparison with **dZ**, **dDiAzep** with a K_i of 430 ± 80 nM was a 20 times more potent inhibitor of recombinantly expressed hCDA but it did not reach the K_i of 25 nM against human liver CDA reported forty years ago for the diazepinone riboside.[36] It is plausible that different sugar puckering of ribose and 2′-deoxyribose had an effect here, as well as a different source of hCDA enzyme. The use of **dDiAzep** instead of dC in the loop of a DNA hairpin led to an A3A inhibitor with nM potency, exhibiting at least 70 times tighter binding to A3A than a dC-hairpin if their K_i and K_m values are compared. However, the inhibitory effect of this nucleoside against hCDA was substantially higher (K_m/K_i = 512, Table 2). This may be due to the differences in the π–π interactions of **dDiAzep** with Phe and Tyr because the binding energy of π–π interactions depends on interacting pairs.[58]

As a control for the evaluation of **dDiAzep** in the structure of a DNA hairpin, we synthesised and tested an FdZ-hairpin that showed powerful inhibition of wild-type A3A with a K_i of 117 nM.[43] Full characterisation of this compound and its crystal structure with wild-type A3A will be published elsewhere.[43]

Unfortunately, due to chemical difficulties we had to abandon the synthesis of the 2′-deoxy form of **dDiAzep-OH** (Fig. 1B). Instead, we synthesised the *R* and *S* isomers of 1,3-diazepine-2-one 2′-deoxyriboside in which the N3 atom is replaced with CH_2. The replacement of the nitrogen atom by CH_2 might be a reason for a considerable decrease in the inhibitory potential of nucleosides against hCDA and engineered $A3B_{CTD}$. However, the *S*-isomer was more potent than the *R*-isomer against both hCDA and engineered $A3B_{CTD}$. Very recently, using X-ray crystallography it was revealed that **FdZ** and **dZ** form tetrahedral intermediates (4-(*R*)-hydroxy-3,4-dihydro-2′-deoxy-5-fluorozebularine and 4-(*R*)-hydroxy-3,4-dihydro-2′-deoxyzebularine) in the enzyme's active site with wild-type A3A[42,43] and catalytically active C-terminal domain of A3G.[59] The position of OH in hydrated **FdZ** and **dZ** is the same in the complex with CDA and A3 with carbon C4 having *R*-stereochemistry. Considering that the nomenclature changes

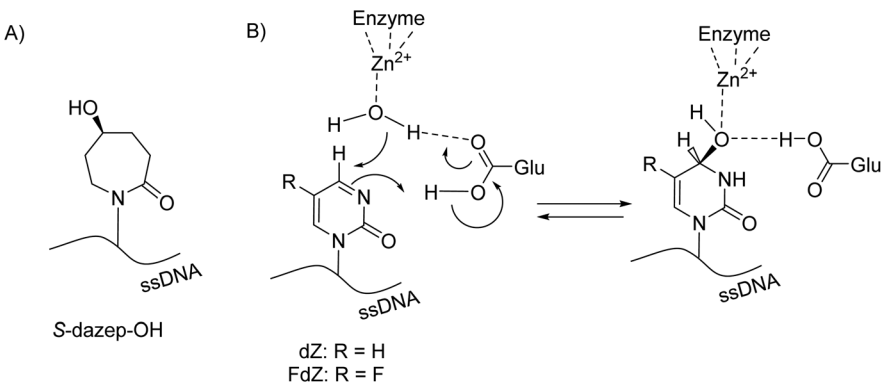

Fig. 7 (A) Chemical structure of ***S*-dAzep-OH** in ssDNA; (B) hydration of **FdZ** and **dZ** by A3 results in 4-(*R*)-hydroxy-3,4-dihydro-2′-deoxyzebularines.

when we replace N3 in 1,3-diazepin-2-one to CH_2 in azepin-2-one (Fig. 3), our observation that the *S*-isomer is more active than the *R*-isomer for 5-hydroxy-azepin-2-ones is consistent with the same conformation seen for the *S*-isomer in the model (Fig. 7A) and for the hydrated **FdZ** in the crystal structure (Fig. 7B).[43] This observation also implies that the 5-hydroxy group of ***S*-dAzep-OH** coordinates to Zn^{2+} and possibly displaces a water molecule that is usually coordinated to Zn^{2+} in A3's active site (Fig. 7).

In the past, high-throughput screening efforts led to the identification of covalent small molecule A3G inhibitors with low micromolar potencies.[60,61] During our study two articles have been published on drug discovery efforts to obtain small molecule inhibitors of A3.[62,63] None approaches the nM potency exhibited by our **FdZ** [43] and **dDiAzep**-containing hairpins. This highlights the interest and need for powerful A3 inhibitors. It is gratifying that the 7-membered ring nucleobase upon incorporation into DNA inhibits A3A, which provides another useful scaffold for further development of A3 inhibitors.

4. Conclusion

In this study we developed a synthetic protocol for the synthesis of the 2′-deoxy derivatives of a known CDA inhibitor and a pair of new CDA inhibitors and their facile incorporation into the previously described ssDNA sequence as inhibitors of A3 enzymes. The inhibitor with the double bond (**dDiAzep**) was a powerful inhibitor of hCDA and showed inhibition of wild-type A3A in the nM range when used instead of dC in the hairpin with a short TTC loop. However, its inhibition of A3A was not as powerful as that exhibited by the **FdZ**-containing hairpin.[43] The differences in the inhibitory potential of the *R* and *S* isomers of 2′-deoxyribosides of hexahydro 5-hydroxy-azepin-2-one shed light on the relative stereochemistry of the hydroxyl substituent which is important in the inhibition of CDA and A3. This study therefore provides useful information for future development of mimics of an intermediate and of transition states of cytidine deamination as powerful inhibitors of A3 enzymes.

Author contributions

M. V. K., G. B. J., E. H., and V. V. F. designed the research, M. V. K. and H. M. K. performed the synthesis, and S. H. and H. M. K. performed enzymatic assays. All authors analysed the data, wrote the article, and have read and agreed to the published version of the manuscript.

Conflicts of interest

The authors have filed a patent on single-stranded DNA enzyme inhibitors describing inhibitors created in this work.[42]

Acknowledgements

The NMR, mass spectrometry and X-ray facilities at Massey University and the assistance of Dr Patrick J. B. Edwards, Mr David Lun and Dr Subo Lee are gratefully acknowledged. We thank Prof. Reuben S. Harris (HHMI and University of Texas Health, San Antonio, TX, USA) and members of his cancer research program for many helpful discussions. We are grateful for the financial support provided by the Worldwide Cancer Research (grant 16-1197), Health Research Council of New Zealand – breast cancer partnership (grant 20/1355), Palmerston North Medical Research Foundation, Maurice Wilkins Centre for Molecular Biodiscovery, Massey University Research Fund (MURF 2015, 7003 and RM20734), Kiwi Innovation Network (KiwiNet) and Massey Ventures Ltd (RM22772) and the School of Natural Sciences, Massey University.

References

1 R. S. Harris and J. P. Dudley, *Virology*, 2015, **479–480**, 131–145.
2 T. Izumi, K. Shirakawa and A. Takaori-Kondo, *Mini-Rev. Med. Chem.*, 2008, **8**, 231–238.
3 R. Suspene, M.-M. Aynaud, D. Guetard, M. Henry, G. Eckhoff, A. Marchio, P. Pineau, A. Dejean, J.-P. Vartanian and S. Wain-Hobson, *Proc. Natl. Acad. Sci. U. S. A.*, 2011, **108**, 4858–4863.
4 C. Swanton, N. McGranahan, G. J. Starrett and R. S. Harris, *Cancer Discovery*, 2015, **5**, 704–712.
5 E.-Y. Kim, R. Lorenzo-Redondo, S. J. Little, Y.-S. Chung, P. K. Phalora, I. Maljkovic Berry, J. Archer, S. Penugonda, W. Fischer, D. D. Richman, T. Bhattacharya, M. H. Malim and S. M. Wolinsky, *PLoS Pathog.*, 2014, **10**, e1004281.
6 S. Venkatesan, R. Rosenthal, N. Kanu, N. McGranahan, J. Bartek, S. A. Quezada, J. Hare, R. S. Harris and C. Swanton, *Ann. Oncol.*, 2018, **29**, 563–572.
7 E. K. Law, A. M. Sieuwerts, K. LaPara, B. Leonard, G. J. Starrett, A. M. Molan, N. A. Temiz, R. I. Vogel, M. E. Meijer-van Gelder, F. C. G. J. Sweep, P. N. Span, J. A. Foekens, J. W. M. Martens, D. Yee and R. S. Harris, *Sci. Adv.*, 2016, **2**, e1601737.
8 J. Zou, C. Wang, X. Ma, E. Wang and G. Peng, *Cell Biosci.*, 2017, **7**, 29.
9 E. K. Law, R. Levin-Klein, M. C. Jarvis, H. Kim, P. P. Argyris, M. A. Carpenter, G. J. Starrett, N. A. Temiz, L. K. Larson, C. Durfee, M. B. Burns, R. I. Vogel, S. Stavrou, A. N. Aguilera, S. Wagner, D. A. Largaespada, T. K. Starr, S. R. Ross and R. S. Harris, *J. Exp. Med.*, 2020, **217**, e20200261.
10 C. Durfee, N. A. Temiz, R. Levin-Klein, P. P. Argyris, L. Alsøe, S. Carracedo, A. A. de la Vega, J. Proehl, A. M. Holzhauer, Z. J. Seeman, Y.-H. T. Lin, R. I. Vogel, R. Sotillo, H. Nilsen and R. S. Harris, *bioRxiv*, 2023, DOI: **10.1101/2023.02.24.529970**.

11 A. M. Sieuwerts, S. Willis, M. B. Burns, M. P. Look, M. E. M.-V. Gelder, A. Schlicker, M. R. Heideman, H. Jacobs, L. Wessels, B. Leyland-Jones, K. P. Gray, J. A. Foekens, R. S. Harris and J. W. M. Martens, *Horm. Cancer*, 2014, **5**, 405–413.
12 L. M. Cortez, A. L. Brown, M. A. Dennis, C. D. Collins, A. J. Brown, D. Mitchell, T. M. Mertz and S. A. Roberts, *PLoS Genet.*, 2019, **15**, e1008545.
13 M. Petljak, A. Dananberg, K. Chu, E. N. Bergstrom, J. Striepen, P. von Morgen, Y. Chen, H. Shah, J. E. Sale, L. B. Alexandrov, M. R. Stratton and J. Maciejowski, *Nature*, 2022, **607**, 799–807.
14 P. Jalili, D. Bowen, A. Langenbucher, S. Park, K. Aguirre, R. B. Corcoran, A. G. Fleischman, M. S. Lawrence, L. Zou and R. Buisson, *Nat. Commun.*, 2020, **11**, 2971.
15 J. M. Kidd, T. L. Newman, E. Tuzun, R. Kaul and E. E. Eichler, *PLoS Genet.*, 2007, **3**, 584–592.
16 M. E. Olson, R. S. Harris and D. A. Harki, *Cell Chem. Biol.*, 2018, **25**, 36–49.
17 M. V. Kvach, F. M. Barzak, S. Harjes, H. A. M. Schares, G. B. Jameson, A. M. Ayoub, R. Moorthy, H. Aihara, R. S. Harris, V. V. Filichev, D. A. Harki and E. Harjes, *Biochemistry*, 2019, **58**, 391–400.
18 F. M. Barzak, S. Harjes, M. V. Kvach, H. M. Kurup, G. B. Jameson, V. V. Filichev and E. Harjes, *Org. Biomol. Chem.*, 2019, **17**, 9435–9441.
19 M. V. Kvach, F. M. Barzak, S. Harjes, H. A. M. Schares, H. M. Kurup, K. F. Jones, L. Sutton, J. Donahue, R. T. D'Aquila, G. B. Jameson, D. A. Harki, K. L. Krause, E. Harjes and V. V. Filichev, *ChemBioChem*, 2020, **21**, 1028–1035.
20 M. Liu, A. Mallinger, M. Tortorici, Y. Newbatt, M. Richards, A. Mirza, R. L. M. van Montfort, R. Burke, J. Blagg and T. Kaserer, *ACS Chem. Biol.*, 2018, **13**, 2427–2432.
21 T. Cacciamani, A. Vita, G. Cristalli, S. Vincenzetti, P. Natalini, S. Ruggieri, A. Amici and G. Magni, *Arch. Biochem. Biophys.*, 1991, **290**, 285–292.
22 T. P. Ko, J. J. Lin, C. Y. Hu, Y. H. Hsu, A. H. Wang and S. H. Liaw, *J. Biol. Chem.*, 2003, **278**, 19111–19117.
23 G. K. Schroeder and R. Wolfenden, *Biochemistry*, 2007, **46**, 13638–13647.
24 M. Chen, M. Herde and C. P. Witte, *Plant Physiol.*, 2016, **171**, 799–809.
25 A. Frances and P. Cordelier, *Mol. Ther.*, 2020, **28**, 357–366.
26 R. Z. Mahfouz, A. Jankowska, Q. Ebrahem, X. Gu, V. Visconte, A. Tabarroki, P. Terse, J. Covey, K. Chan, Y. Ling, K. J. Engelke, M. A. Sekeres, R. Tiu, J. Maciejewski, T. Radivoyevitch and Y. Sauntharajah, *Clin. Cancer Res.*, 2013, **19**, 938–948.
27 T. K. Bjånes, L. P. Jordheim, J. Schjøtt, T. Kamceva, E. Cros-Perrial, A. Langer, G. R. de Garibay, S. Kotopoulis, E. McCormack and B. Riedel, *Drug Metab. Dispos.*, 2020, **48**, 153–158.
28 D. Lavelle, K. Vaitkus, Y. Ling, M. A. Ruiz, R. Mahfouz, K. P. Ng, S. Negrotto, N. Smith, P. Terse, K. J. Engelke, J. Covey, K. K. Chan, J. Desimone and Y. Sauntharajah, *Blood*, 2012, **119**, 1240–1247.
29 D. Ferraris, B. Duvall, G. Delahanty, B. Mistry, J. Alt, C. Rojas, C. Rowbottom, K. Sanders, E. Schuck, K.-C. Huang, S. Redkar, B. B. Slusher and T. Tsukamoto, *J. Med. Chem.*, 2014, **57**, 2582–2588.
30 A. A. Patel, K. Cahill, C. Saygin and O. Odenike, *Blood Adv.*, 2021, **5**, 2264–2271.
31 V. E. Marquez, P. S. Liu, J. A. Kelley, J. S. Driscoll and J. J. McCormack, *J. Med. Chem.*, 1980, **23**, 713–715.
32 V. E. Marquez, P. S. Liu, J. A. Kelley and J. S. Driscoll, *J. Org. Chem.*, 1980, **45**, 485–489.
33 V. E. Marquez, K. V. B. Rao, J. V. Silverton and J. A. Kelley, *J. Org. Chem.*, 1984, **49**, 912–919.
34 M. Kim, K. Gajulapati, C. Kim, H. Y. Jung, J. Goo, K. Lee, N. Kaur, H. J. Kang, S. J. Chung and Y. Choi, *ChemComm*, 2012, **48**, 11443–11445.
35 S. J. Chung, J. C. Fromme and G. L. Verdine, *J. Med. Chem.*, 2005, **48**, 658–660.
36 P. S. Liu, V. E. Marquez, J. S. Driscoll, R. W. Fuller and J. J. McCormack, *J. Med. Chem.*, 1981, **24**, 662–666.
37 G. W. Ashley and P. A. Bartlett, *J. Biol. Chem.*, 1984, **259**, 13621–13627.
38 R. M. Cohen and R. Wolfenden, *J. Biol. Chem.*, 1971, **246**, 7561–7565.
39 C. H. Kim, V. E. Marquez, D. T. Mao, D. R. Haines and J. J. McCormack, *J. Med. Chem.*, 1986, **29**, 1374–1380.
40 L. Frick, C. Yang, V. E. Marquez and R. V. Wolfenden, *Biochemistry*, 1989, **28**, 9423–9430.
41 H. M. Kurup, M. V. Kvach, S. Harjes, F. M. Barzak, G. B. Jameson, E. Harjes and V. V. Filichev, *Biochemistry*, 2022, **61**, 2568–2578.
42 F. M. Y. Barzak, V. V. Filichev, E. Harjes, S. Harjes, G. B. Jameson, H. M. Kurup, M. V. Kvach and Y. Su, WO2022162536, 2022.
43 S. Harjes, H. M. Kurup, A. E. Rieffer, M. Bayarjagal, J. Filitcheva, Y. Su, T. K. Hale, V. V. Filichev, E. Harjes, R. S. Harris and G. B. Jameson, *bioRxiv*, 2023, DOI: **10.1101/2023.02.17.528918**.
44 J. C. Serrano, D. von Trentini, K. N. Berrios, A. Barka, I. J. Dmochowski and R. M. Kohli, *ACS Chem. Biol.*, 2022, **17**, 3379–3388.
45 J. J. Barchi, A. Haces, V. E. Marquez and J. J. McCormack, *Nucleosides Nucleotides*, 1992, **11**, 1781–1793.
46 P. S. Liu, V. E. Marquez, J. A. Kelley and J. S. Driscoll, *J. Org. Chem.*, 1980, **45**, 5225–5227.
47 O. R. Ludek, G. K. Schroeder, C. Liao, P. L. Russ, R. Wolfenden and V. E. Marquez, *J. Org. Chem.*, 2009, **74**, 6212–6223.
48 S. Belyakov, B. Duvall, D. Ferraris, G. Hamilton and M. Vaal, WO2010118010, 2010.
49 M. P. Kotick, C. Szantay and T. J. Bardos, *J. Org. Chem.*, 1969, **34**, 3806–3813.
50 E. Tarkin-Tas and L. J. Mathias, *Macromolecules*, 2010, **43**, 968–974.

51 V. Rolland, M. Kotera and J. Lhomme, *Synth. Commun.*, 1997, **27**, 3505–3511.
52 M. Paar, W. Schrabmair, M. Mairold, K. Oettl and G. Reibnegger, *ChemistrySelect*, 2019, **4**, 1903–1908.
53 M. J. Grillo, K. F. M. Jones, M. A. Carpenter, R. S. Harris and D. A. Harki, *Trends Pharmacol. Sci.*, 2022, **43**, 362–377.
54 T. V. Silvas, S. Hou, W. Myint, E. Nalivaika, M. Somasundaran, B. A. Kelch, H. Matsuo, N. K. Yilmaz and C. A. Schiffer, *Sci. Rep.*, 2018, **8**, 7511.
55 S. Hou, T. V. Silvas, F. Leidner, E. A. Nalivaika, H. Matsuo, N. K. Yilmaz and C. A. Schiffer, *J. Chem. Theory Comput.*, 2019, **15**, 637–647.
56 R. Buisson, A. Langenbucher, D. Bowen, E. E. Kwan, C. H. Benes, L. Zou and M. S. Lawrence, *Science*, 2019, **364**, eaaw2872.
57 V. E. Marquez, J. J. Barchi Jr., J. A. Kelley, K. V. Rao, R. Agbaria, T. Ben-Kasus, J. C. Cheng, C. B. Yoo and P. A. Jones, *Nucleosides, Nucleotides Nucleic Acids*, 2005, **24**, 305–318.
58 K. A. Wilson, J. L. Kellie and S. D. Wetmore, *Nucleic Acids Res.*, 2014, **42**, 6726–6741.
59 A. Maiti, A. K. Hedger, W. Myint, V. Balachandran, J. K. Watts, C. A. Schiffer and H. Matsuo, *Nat. Commun.*, 2022, **13**, 7117.
60 M. Li, S. M. D. Shandilya, M. A. Carpenter, A. Rathore, W. L. Brown, A. L. Perkins, D. A. Harki, J. Solberg, D. J. Hook, K. K. Pandey, M. A. Parniak, J. R. Johnson, N. J. Krogan, M. Somasundaran, A. Ali, C. A. Schiffer and R. S. Harris, *ACS Chem. Biol.*, 2012, **7**, 506–517.
61 M. E. Olson, M. Li, R. S. Harris and D. A. Harki, *ChemMedChem*, 2013, **8**, 112–117.
62 J. J. King, F. Borzooee, J. Im, M. Asgharpour, A. Ghorbani, C. P. Diamond, H. Fifield, L. Berghuis and M. Larijani, *ACS Pharmacol. Transl. Sci.*, 2021, **4**, 1390–1407.
63 Y.-H. Zhang, X.-C. Guo, J.-B. Zhong, D.-X. Zhong, X.-H. Huang, Z.-Y. Fang, C. Zhang and Y.-J. Lu, *ChemistrySelect*, 2022, **7**, e202201456.